GaHV-2 ICP22 protein is expressed from a bicistronic transcript regulated by three GaHV-2 microRNAs

Boumart, Imane; Figueroa, Thomas; Dambrine, Ginette; Muylkens, Benoît; Pejakovi, Srdan; Rasschaert, Denis; Dupuy, Catherine

Published in:
The Journal of general virology

DOI:
10.1099/jgv.0.001124

Publication date:
2018

Document Version
Publisher's PDF, also known as Version of record

JOURNAL OF GENERAL VIROLOGY

RESEARCH ARTICLE

Boumart *et al.*, *Journal of General Virology* 2018;99:1286–1300

DOI 10.1099/jgv.0.001124

MICROBIOLOGY SOCIETY

GaHV-2 ICP22 protein is expressed from a bicistronic transcript regulated by three GaHV-2 microRNAs

Imane Boumart,[1] Thomas Figueroa,[1]† Ginette Dambrine,[1] Benoit Muylkens,[2] Srdan Pejakovic,[2] Denis Rasschaert[1,*] and Catherine Dupuy[1]

Abstract

Herpesviruses have a lifecycle consisting of successive lytic, latent and reactivation phases. Only three infected cell proteins (ICPs) have been described for the oncogenic Marek's disease virus (or Gallid herpes virus 2, GaHV-2): ICP4, ICP22 and ICP27. We focus here on ICP22, confirming its cytoplasmic location and showing that *ICP22* is expressed during productive phases of the lifecycle, via a bicistronic transcript encompassing the *US10* gene. We also identified the unique promoter controlling *ICP22* expression, and its core promoter, containing functional responsive elements including E-box, ETS-1 and GATA elements involved in *ICP22* transactivation. *ICP22* gene expression was weakly regulated by DNA methylation and activated by ICP4 or ICP27 proteins. We also investigated the function of GaHV-2 ICP22. We found that this protein repressed transcription from its own promoter and from those of IE ICP4 and ICP27, and the late gK promoter. Finally, we investigated posttranscriptional ICP22 regulation by GaHV-2 microRNAs. We found that mdv1-miR-M5-3p and -M1-5p downregulated *ICP22* mRNA expression during latency, whereas, unexpectedly, mdv1-miR-M4-5p upregulated the expression of the protein ICP22, indicating a tight regulation of *ICP22* expression by microRNAs.

INTRODUCTION

Gallid herpes virus 2 (GaHV-2) is an oncogenic avian herpesvirus that causes paralysis due to the infiltration of mononuclear cells into the peripheral nerves, and T-cell lymphoma in chickens. Like all herpesviruses, GaHV-2 has a lifecycle divided into lytic and latent phases, the latent phase being associated with oncogenesis [1]. According to the Cornell model, GaHV-2 infection in chickens is initiated by early semi-productive cytolytic infection in B cells, peaking 3 to 7 days post-infection (p.i.) in experimental conditions [2]. Latency, the second major phase of the viral lifecycle, begins at about 7 days p.i. and is characterized by the maintenance of the viral genome without productive replication in $CD4^+$ T cells, resulting in oncogenesis. Viral lytic genes are repressed during latency, whereas the viral non-coding RNAs, including the latency-associated transcript (LAT) and microRNAs, continue to be expressed [3, 4]. As reported for other herpesviruses, latent GaHV-2 in lymphocytes can revert to semi-productive cytolytic replication, in a process known as reactivation, after 2 to 3 weeks, whereas productive lytic replication occurs in the epithelial cells of feather follicles [2].

The replication of GaHV-2 viral particles during the lytic phase begins with the expression of three immediate early (IE) genes conserved among alphaherpesviruses: *ICP4*, *ICP22* and *ICP27* [1]. In all herpesviruses, the IE genes are expressed in a classical tightly regulated temporal cascade [5–8]. The GaHV-2 *ICP22* gene is located at the 5′ end of the unique short (U_S) region, as in most alphaherpesviruses; it encodes a 179-amino acid protein [9]. BLAST-P analysis has shown that GaHV2-ICP22 possesses the core HERPES_IE68 domain known to be well-conserved among other previously described alphaherperviruses ICP22 [10]. This core domain is lacking from the Iltovirus genus (GaHV-1),

Received 9 February 2018; Accepted 5 July 2018

Author affiliations: [1]Equipe Transcription et Lymphome Viro-Induit (TLVI), UMR 7261 CNRS, Université François Rabelais de Tours, UFR Sciences et Techniques, Parc de Grandmont, 37200 Tours, France; [2]Veterinary Integrated Research Unit, Faculty of Sciences, Namur Research Institute for Life Sciences (NARILIS), University of Namur (UNamur), 5000 Namur, Belgium.

***Correspondence:** Denis Rasschaert, denis.rasschaert@univ-tours.fr

Keywords: GaHV-2; alphaherpesvirus; ICP22; transcription regulation; translation regulation; microRNA.

Abbreviations: Ab, antibody; AnHV, anatid herpesvirusc; BGSA, bisulfite genomic sequencing analysis; BoHV-1, bovine herpesvirus 1; CEF, chicken embryo fibroblasts; CoHV, Colombine herpesvirus; CMV, cytomegalovirus; CS, chicken serum; dpi, days post-infection; E, early; EHV-1, equine herpesvirus 1; FCS, fetal calf serum; GaHV-1-GaHV-2, gallid herpesvirus 1-2; HHV-1, 3, 5, human herpes virus 1, 3, 5; ICP4, 22, 27, infected cell protein 4, 22, 27; IE, immediate early; Inr, initiator element; IRS, internal repeat short; L, late; LAT, latency-associated transcript; lncRNA, long non-coding RNA; MCMV, murine cytomegalovirus; MD, Marek's Disease; MeHV, Meleagrid herpesvirus; miRNA, microRNA; miRE, mRNA decay; PBL, peripheral blood leucocytes; PTC, premature sphenicid herpesvirus; SuHV-1, Suid herpes virus-1; TRL, terminal repeat long; TRS, terminal repeat short; TSS, transcription start site; UL, unique long; US, unique short; UTR, upstream terminal region; VP, viral protein.

†**Present address:** Interactions Hôtes Agents Pathogènes, Université de Toulouse, INRA, ENVT, Toulouse, France.

which seems to have no *ICP22* homologue, despite having a a similarly organized U_S region in its genome.

Initially described as an IE gene [11], GaHV-2 *ICP22* has since been shown to be a late (L) gene [12, 13]. Indeed, whereas *ICP4* and I*CP27* are clearly true IE genes regardless of the herpesvirus strain, there is no consensus regarding the temporal pattern of *ICP22* expression. Indeed, *ICP22* has been described as an IE gene in HHV-1 and HHV-3, but appears to be a non-IE gene in SuHV-1 [14] and both an IE and L gene in BoHV-1 [15, 16].

By isolating GaHV-2 deletion mutants lacking *ICP22*, *ICP22* was found to be dispensable for viral replication in cultured cells and for *in vivo* chicken infection by an attenuated strain of GaHV-2 [13], whereas highly virulent GaHV-2 RB-1B mutants lacking ICP22 had lower replication rates in cultured cells but were still able to induce MD lymphomas, with lower rates of early cytolytic infection, tumour incidence and mortality, suggesting a requirement of ICP22 for the lytic replication of GaHV-2, rather than latency [12]. The GaHV-2 RB-1B mutant can be reactivated from lymphoma-derived lymphoblastoid cell lines, demonstrating that GaHV-2 ICP22 is dispensable for reactivation [17]. However, the precise role of ICP22 in GaHV-2 pathogenesis remains to be determined.

HHV-1 ICP22 is the best studied of the alphaherpesvirus ICP22 homologue. It has been shown to play an important role in efficient viral replication and pathogenesis, through the modulation of HHV-1 gene expression, by repressing E gene transcription or enhancing L gene transcription [18–20]. Most ICP22 homologues have been shown to modulate the transcription of viral genes [16, 21], thereby affecting the herpesvirus lifecycle. The ICP22 homologue of HHV-3 (ORF63), for example, downregulates transcription of the homologue of ICP4, IE62, and thus plays a key role in the establishment of latent infection [22]. The ICP22 homologue of equine herpesvirus type 1 (EHV-1) can transactivate EHV-1 promoters either alone or in combination with other regulatory proteins of EHV-1, including ICP4 and ICP27 homologues, in reporter gene assays [23]. Studies in a heterologous system have shown that GaHV-2 ICP22 transactivates the ICP27 promoter in combination with ICP4 [24], but this observation has yet to be confirmed in the natural chicken system.

Completion of the GaHV-2 lifecycle requires fine-tuning of each of the component phases. We therefore investigated the regulation of GaHV-2 ICP4 and ICP27 expression in more detail, as these two proteins are principally involved in the switch between the latent and productive phases [7, 25, 26]. GaHV-2 ICP4 and ICP27, which are expressed under the control of two alternative promoters, were specifically downregulated by mdv1-miR-M7-5p, one of the miRNAs of the mdv1-miR-M8-M10 cluster mapping to the first LAT intron [25]. Indeed, as explained in the recent review by Sorel and Dewals [27], herpesvirus miRNAs downregulate IE transactivators, thereby restricting the lytic phase and promoting latency and long-term persistence. In addition, herpesvirus miRNAs may contribute to the proliferation and transformation of latently infected cells. In this context, GaHV-2 mdv1-miR-M4-5P, an orthologue of cellular gga-miR-155-3P, is one of the most reliable models. The mdv1-miR-M4-5P has been shown to downregulate the same cellular targets as its gga-miR-155-3P orthologue, suggesting that both may be involved in cell transformation and oncogenesis [28, 29]. The deletion of mdv1-miR-M4 has been shown to abolish the induction of lymphomas in chicken, providing the first demonstration of a role for a viral miRNA in oncogenesis in a natural model *in vivo* [30]. GaHV-2 mdv1-miR-M4 has also been shown to target the viral UL28 and UL32 genes [29]. The mdv1-miR-M4 miREs are located in coding regions, like those of mdv1-miR-M7 [25, 29], rather than in 3′-UTR sequences, as usually observed for animals. Moreover, the complexity of viral miRNA functions has been highlighted in various studies reporting the presence of viral miRNAs in HHV-4 virions, suggesting a role in controlling the early steps of infection [31], or that unusual targeting within the 5′-UTR mRNA can occur with a viral miRNA encoded by HHV-5 [32].

In this study, we characterized the GaHV-2 *ICP22* gene, its expression and regulation during the lytic, latent and reactivation phases of the GaHV-2 viral cycle. We confirmed from the finding of Parcells *et al.* [12, 13] that the Icp22 protein is present essentially in the cytoplasm of the infected cells, and showed that *ICP22* is expressed during the lytic phase of the GaHV-2 lifecycle, through a bicistronic transcript encompassing the *US10* gene. We also showed that the expression of this gene was controlled by a unique promoter, and we identified the core promoter and functional regulatory elements. We assessed the transcriptional and posttranscriptional regulation of *ICP22* expression in more detail. We found that *ICP22* gene expression was weakly regulated by DNA methylation. It was also activated by the ICP4 and ICP27 proteins and repressed by ICP22 itself. ICP22 has also been shown to act as a repressor for other GaHV-2 genes. Finally, we investigated the targeting of ICP22 by GaHV-2 microRNAs and showed that mdv1-miR-M5-3p and –M1-5p downregulated *ICP22* expression, as generally observed, whereas, surprisingly, mdv1-miR-M4-5p upregulated *ICP22* expression.

RESULTS

ICP22 expression is associated with the lytic phase of the lifecycle

We first investigated the intracellular distribution of ICP22 by staining RB-1B GaHV-2-infected chicken embryo fibroblasts (CEF RB-1B) and MSB-1 cells latently infected with GaHV-2 with an anti-ICP22 polyclonal antiserum. In parallel, we used mAb 3F19, directed against the major capsid protein VP5 [33], which is produced exclusively during the lytic and reactivation phases (Fig. 1a). In CEF RB-1B cells, corresponding to the lytic phase of infection, ICP22 was detected mostly in the cytoplasm of the infected cells,

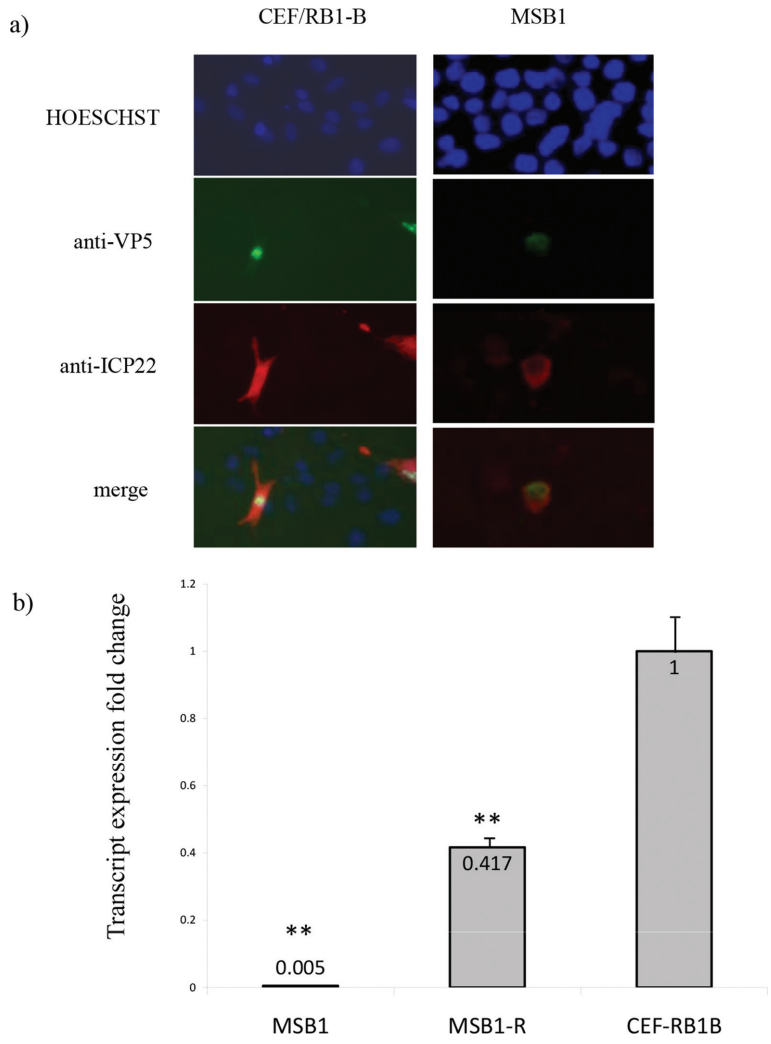

Fig. 1. Expression of *ICP22* in cells with lytic or latent infection. (a) Cellular distribution of ICP22 in CEF RB-1B and MSB-1 cells. ICP22 proteins were labelled with polyclonal antibodies against ICP22 and Alexa Fluor 594–goat anti-rabbit IgG (red), and VP5 was labelled with the anti-VP5 mAb 3F19 and Alexa Fluor 488–goat anti-mouse IgG (green). Cell nuclei were stained with Hoechst stain (top). (b) Relative levels of ICP22 mRNAs in MSB-1 cells, MSB-1 cells treated with 3 mM sodium *n*-butyrate (MSB-1R) and RB-1B-infected CEFs (CEF RB-1B). Total RNA was isolated for reverse transcriptase (RT)-qPCR with the B264-A962 primers. The relative levels of ICP22 mRNA were determined by the $2^{-\Delta\Delta Ct}$ method, with normalization relative to GAPDH mRNA. The reported values are expressed relative to that for CEF RB-1B, arbitrarily set to 1. The histograms correspond to the mean of triplicates for two independent experiments. Standard errors are shown. Significant differences in expression are indicated with asterisks (**), for Student's *t*-test *P*-value<0.01.

whereas, as expected, the major capsid protein VP5 was found exclusively in the nucleus. In latently infected MSB-1 lymphocytes, ICP22 was found only in the cytoplasm of cells expressing VP5 representing naturally reactivated cells (approximately 1 % of total cells).

We estimated ICP22 mRNA levels during the lytic and latent phases of the GaHV-2 cycle, by quantitative RT-PCR with the B264/A962 primer pair, on total mRNA extracted from MSB-1 cells, MSB-1 cells treated with sodium *n*-butyrate (MSB-1R) to induce reactivation of the latent virus, and CEF RB-1B cells. We found that *ICP22* was transcribed exclusively during lytic phases, with mRNA levels during the lytic phase proper 2.5 times higher than those during reactivation (Fig. 1b). The very low levels of ICP22 transcript in latently infected MSB-1 cells is consistent with previous immunofluorescence (IF) observations that revealed ICP22 to be present only in MSB-1 cells in which the latent GaHV-2 virus had been naturally reactivated.

ICP22 is a part of a lytic bicistronic transcript

We characterized the ICP22 mRNA, by 5′ and 3′ RACE on the total RNA extracted from MSB-1 cells, MSB-1R and CEF RB-1B cells. Six independent libraries were constructed in pGEMTeasy, by cloning the 5′ and 3′ RACE PCR products amplified with the A960 primer binding 41 nt

downtream from the start codon and the A478 primer binding 131 nt upstream from the *ICP22* stop codon, respectively. We sequenced 50 clones from each library. For 5′ RACE PCR, we identified two TSSs: a major TSS_{155440} 41 nt upstream from the *ICP22* start codon, which was found in 70 to 75 % of the clones of the three cell lines, and a minor site, TSS_{155424}, located 16 nt upstream from the major TSS. The major TSS corresponds to adenosine A 155440 of the RB-1B genome, the first adenosine residue of a canonical predicted initiator element (Inr) TTACACT (Fig. 2a).

For 3′ RACE we identified two 3′ end sites. The very minor site (nt 156289) located 12 nt downstream from an ATTAAA polyA signal was found in only one clone of the MSB-1R and RB-1B-infected CEF libraries (Fig. 2a). The use of this minor site would lead to the production of an mRNA specific to ICP22. The second 3′ end site

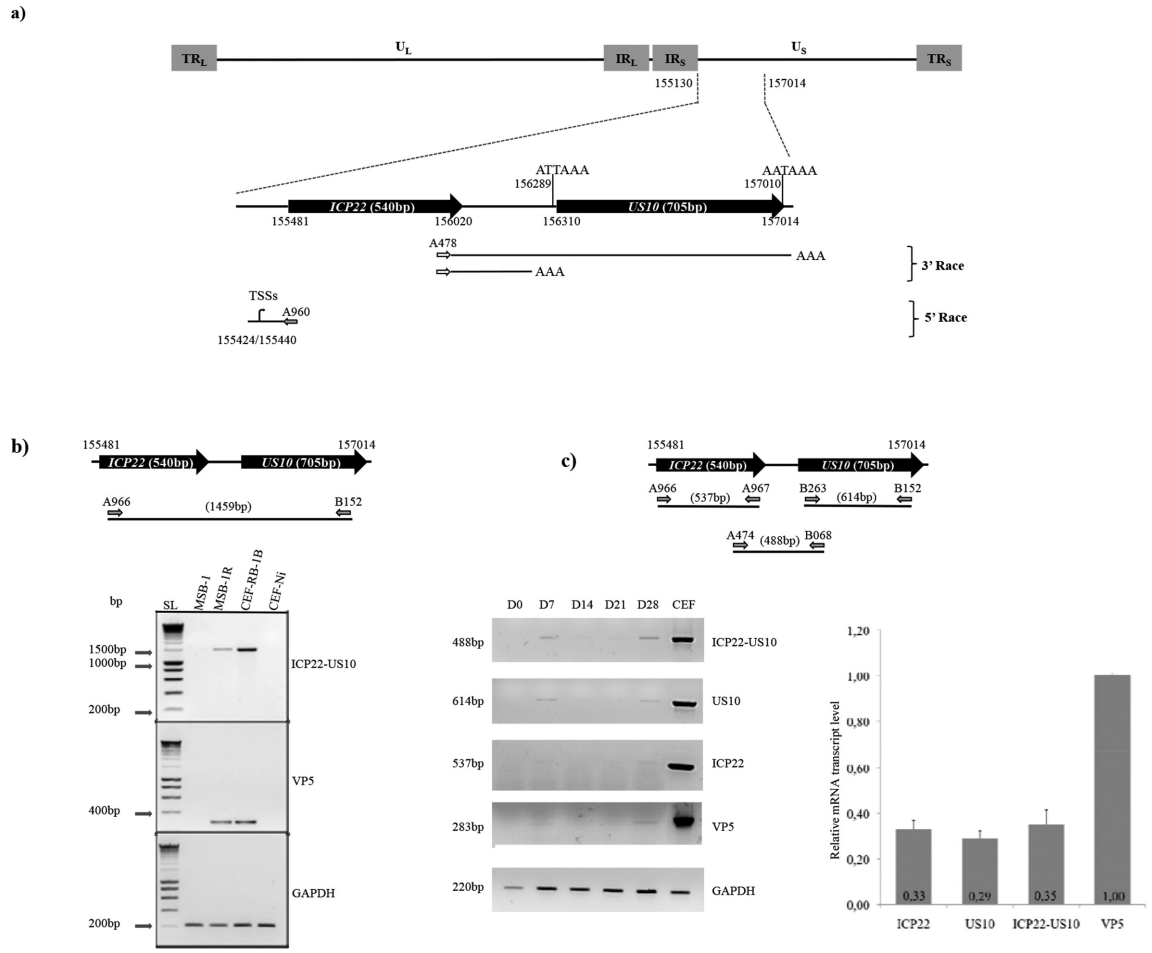

Fig. 2. Characterization of the transcripts encoded by the *ICP22* and *US10* locus. (a) Schematic diagram of the TRL/TRS regions of the GaHV-2 RB1B strain genome (GenBank accession no. EF523390.1) (top), expanded to show a part of the U_S region (155130–157014) in detail. Black arrows show the predicted ORF; the numbers indicate the location relative to the GaHV-2 RB-1B genome. Bottom: identification of the 3′ (AAA) and 5′ ends of ICP22 byh RACE-PCR with RNA extracts from MSB-1 cells, MSB-1 cells after reactivation with 3 mM sodium *n*-butyrate (MSB-1R) and CEF RB-1B cells. White and grey arrows indicate the positions of the primers used for 3′′RACE-PCR (A478) and for 5′ RACE-PCR (A960), respectively. The position of the predicted polyA signal is indicated. (b) Identification, by semi-quantitative RT-PCR, of ICP22-US10, with the A966 and B152 primers, GAPDH and VP5 transcripts in unifected CEFs, CEF RB-1B, MSB-1 and MSB-1R cells. (c) Identification, by semi-quantitative RT-PCR, of ICP22, US10 and ICP22-US10 GAPDH and VP5 transcripts from RNA extracts from the peripheral blood leukocytes of chickens infected with RB1B for 28 days, on days 0 (D0), 7 (D7), 14 (D14), 21 (D21) and 28 (D28). Left: migration of the 488 bp amplicon (primers A474-B068), the 614 bp amplicon (primers B263-B152), the 537 bp amplicon (primers A966-A967), the 283 bp amplicon for VP5 (432–433 primers) and the 220 bp amplicon for GAPDH (primers M450–M451). Right: ratios of each band of the RT-PCR products obtained in RB-1B-infected CEF were determined by comparing the relative peak areas of the amplifications, with Adobe Photoshop 6 standardized with those obtained with GAPDH and normalized with respect to VP5. The intensity of each fragment was standardized according to amplicon length and the intensity of the band corresponding to GAPDH, and normalized against VP5, for which the value was arbitrarily set to one. Error bars indicate the SEM for three independent biological experiments.

(nt 157010), found in all the other sequenced clones, is located downstream from the *US10* stop codon, 19 nt downstream from a canonical AATAAA polyA signal (Fig. 2a). Finally, RT-PCR on the total RNA extracted from the three types of cells with the A966 and B152 primers encompassing both *ICP22* and *US10* confirmed the presence of *ICP22* and *US10* in a large bicistronic transcript during the lytic and reactivation phases (Fig. 2b).

For confirmation of these data *in vivo*, we carried out a set of three semi-quantitative PCRs on total RNA extracted from peripheral blood leucocytes (PBLs) collected at 0, 7, 14, 21 and 28 days p.i. from chickens infected with GaHV2 RB-1B using CEF RB-1B as a control. The A966 and A967, B263 and B152, and A474 and B068 primer pairs were used for more specific amplification of the *ICP22* and *US10* genes and the bicistronic mRNA, respectively, yielding amplicons of similar length (Fig. 2c). The levels of *ICP22*, *US10* and the bicistronic mRNA differed significantly between lytic phases of infection (7 and 28 days p.i.) and the latent phase of viral infection (14 and 21 days p.i.) (Fig. 2c). The very weak bands on electrophoretic gels at 14 and 21 days p.i. may reflect the viral reactivation classically reported in this *in vivo* model. The intensity of each band for RB-1B-infected CEFs was standardized with respect to a band corresponding to GAPDH amplified with the GAPDH-F and GAPDH-R primers and normalized with respect to VP5 (Fig. 2c). No significant differences were observed between the three amplicons. We therefore conclude, consistently with our 3′ RACE results, that the *ICP22* and *US10* transcripts were essentially produced as a single bicistronic mRNA during the lytic phase of the viral cycle.

The *ICP22* core promoter is controlled by at least seven response elements

We characterized the *ICP22* core promoter, with a nested set of four truncated constructs encompassing the 1000 nt upstream from TSS_{155440}. The 1000, 800, 500, 200 and 100 nt immediately upstream from the start codon were amplified and inserted into the pGL3-basic vector to obtain the pICP22-1000, pICP22-800, pICP22-500, pICP22-200 and pICP22-100 constructs, respectively (Fig. 3a). MSB-1 cells were cotransfected with these promoter constructs, the pGL3-basic vector (negative control) or pcDNA-MLuc (positive control sharing the CMV promoter), together with the pRL-TK vector (*Renilla* luciferase), and the resulting promoter activity was assessed in luciferase assays. The ratio of firefly/*Renilla* luciferase activities for each template was arbitrarily expressed relative to that for the longest construct (pICP22-1000). Unlike the pGL3-basic control and pICP22-100, the other four promoters were efficient (Fig. 3a), with pICP22-200 having the highest levels of activity, 46 % that of the standard CMV promoter of pcDNA-MLuc (data not shown). We therefore identified pICP22-200 as the minimal functional core promoter.

In silico analysis of the pICP22-200 core promoter with Genomatix software revealed the presence of response elements (REs) for basal transcription, TATA and GC boxes, and five REs potentially involved in the regulation of gene transcription during haematopoiesis, an Ebox, GATA box and REs for Oct-1, CRE and Ets-1. The seven predicted REs were mutated separately in the pICP22-200 core promoter construct. The resulting constructs were used to transfect MSB-1 cells and the corresponding measured luciferase activities were standardized against the native pICP22-200 (Fig. 3b). All seven REs seemed to be involved in ICP22 promoter activity. The TATA and GATA boxes, and the ETS-1RE, E-box and GC box, mutations of which decreased luciferase activity significantly, by 27, 47, 55, 91 and 32 %, respectively, were involved in the activation of *ICP22* transcription, whereas, Oct-1 and CRE, mutations of which increased luciferase activity by 29 and 43 %, respectively, were involved in its repression.

The *ICP22* core promoter is not regulated by DNA methylation

We investigated pICP22-200 promoter methylation by bisulfite genomic sequencing analysis (BGSA) of viral genomic DNA extracted from MDV-infected cells in the three phases of the viral lifecycle: MSB-1 cells (latency), MSB-1 cells treated with 5-azacytidine (MSB-1R) for reactivation and RB-1B-infected CEFs (lytic phase) (Fig. 3c). The five cytosine/guanine (CpG) dinucleotides of the pICP22-200 promoter were unmethylated (MSB-1 cells) or slightly methylated (MSB-1R and CEF RB-1B), with the RE USF-1 Ebox, in particular, being methylated during the reactivation phase (28 %) and the lytic phase (14 %).

ICP22 gene expression is regulated by three GaHV-2 miRs

An internal BLAST search predicted the presence of three potential miRNA responsive elements (miREs), for mdv1-miR-M5-3p, mdv1-miR-M4-5p and mdv1-miR-M1-5p, within the ICP22 ORF. There was a miRE-M5-3p (position 155496–155518) 15 nt upstream from the start codon, a miRE-M1-5p (position 155786–155807) 656 nt upstream from the start codon, and a miRE-M4-5p (position 155998–156020) spanned the stop codon (Fig. 4a). The relative expression levels of the three miRNAs mdv1-miR-M5-3p, mdv1-miR-M4-5p and mdv1-miR-M1-5p, in CEF RB-1B, MSB-1 and MSB-1R cells, have been estimated from the RNA extracted for the determination of the ICP22-mRNA level of the Fig. 1, by specific RT-qPCRs with the primers M1-5p, M4-5p and M5-3p, respectively (Fig. 4b). The expression of mdv1-miR-M1-5p was significantly reduced (five times) during the reactivation phase. The expression of mdv1-miR-M4-5p increased threefold in the latently infected MSB-1 cells. Lastly, mdv1-miR-M5-3p, which was 16 times more expressed in MSB-1 than in lytic-infected CEF RB-1B cells, was very weakly detected during the reactivation phase.

We investigated the functions of the miREs, by inserting the predicted ICP22 ORF into the pcDNA3.1 expression vector, to generate pcICP22 and three mutants constructs: pcICP22-miRE-M1m, pcICP22-miRE-M5m and pcICP22-miRE-M4m

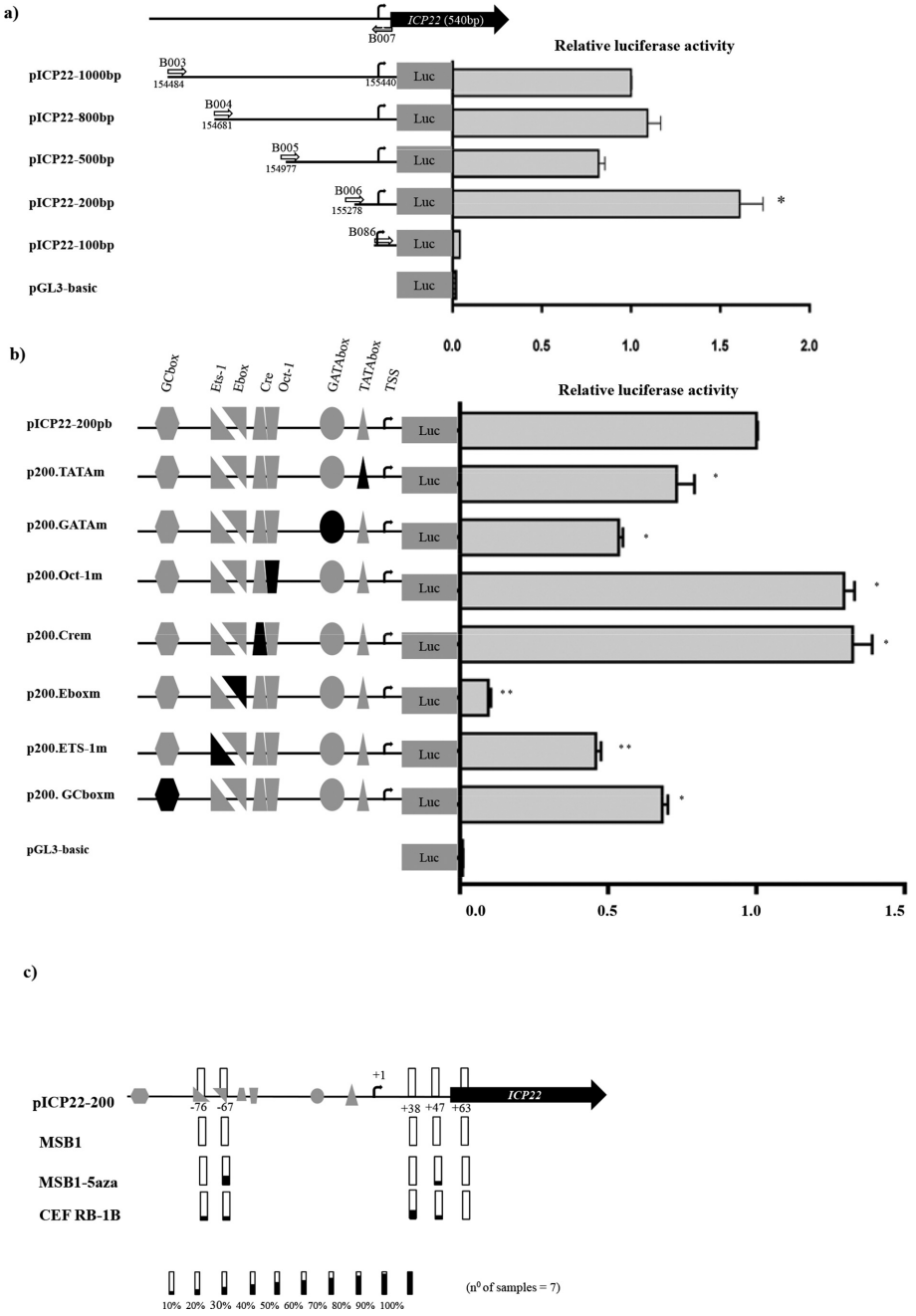

Fig. 3. Characterization of the *ICP22* promoter. (a) Characterization of the core promoter of *ICP22* in MSB-1 cells. Schematic diagram of the four promoter deletion constructs inserted downstream from the firefly gene (Luc) in the pGL-3 Basic vector, with numbers indicating nt positions relative to the RB-1B genome (GenBank accession no. EF523390.1). Promoter activity was assessed by measuring luciferase assay after the transfection of MSB-1 cells. Data are expressed relative to luciferase activity after arbitrary normalization against the p*ICP22*-1000 promoter, for which the value was set to 1. Error bars indicate the SEM for three independent biological experiments performed in triplicate (n=3). *P<0.05 in Student's t-test. (b) Identification of the response elements (REs) involved in regulation of the pICP22-200 core construct. The REs identified *in silico* with Genomatix software are indicated by grey shapes, and the mutated REs are indicated by darker shapes. The promoter activities of the mutated-RE constructs were assessed in luciferase assays on MSB-1 cells. Luciferase activities were normalized with respect to that for pICP22-200, set to 1. Error bars indicate the SEM for three independent biological experiments performed in triplicate. *Student's t-test P-value<0.05 versus pICP22-200 and ** P-value<0.001 versus pICP22-200. (c) DNA methylation of the pICP22-200 promotor. Methylation status of CpG islands (CGI) in the pICP22-200 promoter region, determined in three cell conditions: MSB-1, MSB-1 treated with 5-azacitidine (MSB-1R) and CEF RB-1B. The white rectangles correspond to the CGIs identified in this region, according to the TSS2 annotation. The unmethylated CGIs are shown as white rectangles/boxes, methylated CGIs are indicated by black rectangles. The mean percent methylation is indicated by the black rectangles.

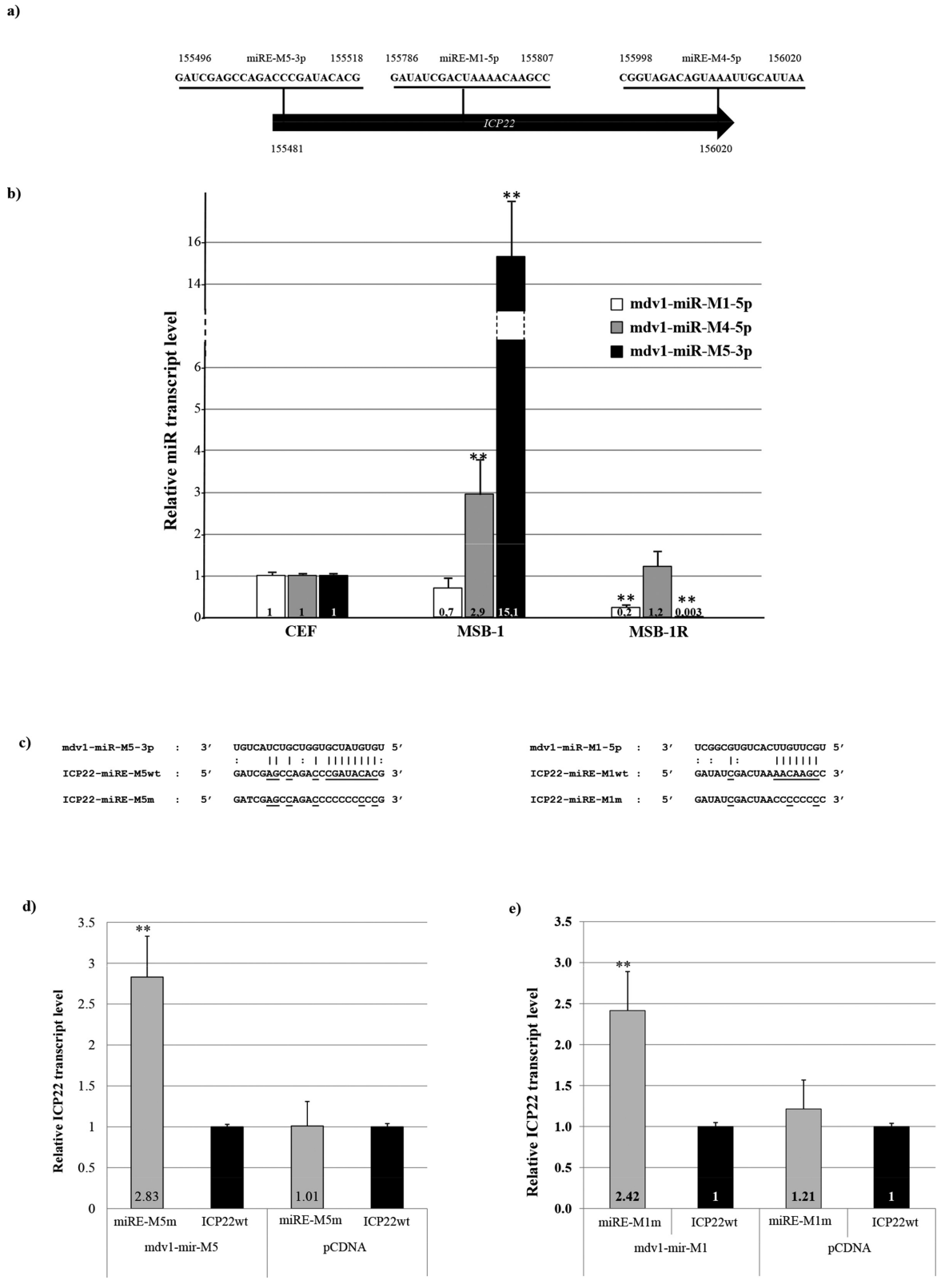

Fig. 4. Targeting of ICP22 by mdv1-miR-M5-3p and mdv1-miR-M1-5p. (a) Localization of the miRE-M5-3p, miRE-M1-5p and miRE-M4-5p in *ICP22* gene. The position of each miRE is indicated. (b) Relative expression of mdv1-miR-M1-5P (white), mdv1-miR-M4-5P (grey) and mdv1-miR-M5-3P (black), in CEF RB-1B, MSB-1 and MSB-1R cells as determined by RT-qPCR with the $2^{-(\Delta\Delta Ct)}$ method using U6snRNA as the reference. Error bars of two independent experiments carried out in triplicate are shown. For each miR, the values

are standardized to CEF RB-1B values, arbitrarily set to 1. Significant differences in expression are indicated with asterisks (**), for Student's *t*-test $P<0.01$. (c) The sequence complementarity of mdv1-miR-M5-3p (left), and mdv1-miR-M1-5p (right) and their predicted miREs identified in the *ICP22* sequences of the GaHV-2 RB1B genome are shown. The microRNA seed region is highlighted in black (: denotes wobble pair G-U, **I** denotes Watson–Crick pair); bars indicate nucleotides complementary between the miR and the corresponding miRE. ICP22-miRE-M5m and ICP22-miR-M1m are the sequences of the related mutated miRE with the changed nucleotide and complementarities. (d–e) Downregulation of the ICP22 transcript by mdv1-miR-M5-3p and mdv1-miR-M1-5p. DF-1 cells were cotransfected with pcDNA constructs, pcICP22 (ICP22wt) or pcICP22 with a mutated miRE-M5-3p (miRE-M5m) or miR-M1-5p (miRE-M1m), and with miRNA expression vector: pcDNA-mdv1-miR-M5-3p, pcDNA-mdv1-miR-M1-5p, or the empty pcDNA vector as a control. Total RNA was extracted and subjected to RT-qPCR. ICP22 transcript levels were calculated relative to those of GAPDH. ICP22 mRNA levels were quantified by the RT-qPCR $2^{-\Delta\Delta Ct}$ method, with GAPDH mRNA as the reference. The histograms show the mean of triplicates of two independent lipofections of DF-1 cells. ICP22 mRNA levels were normalized relative to those after transfection with pCDNA3.1. * Student's *t*-test, *P*-value<0.05 versus pCDNA3.1.

(Figs 4b and 5a). As miRE-M4-5p spanned the stop codon, we took care to ensure that the UAA codon was conserved in the pcICP22-M4m construct (Fig. 5a). These constructs were used to contransfect GaHV-2-free cells (DF-1 cells), with pcDNA-mdv1-miR-M1, pcDNA-mdv1-miR-M5 or pcDNA-mdv1-miR-M4, each expressing the premiR, or native pcDNA.3.1 as a negative control. Total RNA was extracted from the DF-1 cells 48 h after transfection, and ICP22 mRNA levels were estimated directly, by RT-qPCR. Mutations of miRE-M5-3p and miRE-M1-5p were associated with significant increases in ICP22-mRNA level, of 2.8- and 2.4-fold, respectively (Fig. 4d, e). Surprisingly, the mutation of miRE-M4-5p decreased ICP22 mRNA levels by about 50 %, revealing a positive impact of mdv1-miR-M4-5p on *ICP22* expression (Fig. 5b). For confirmation of these findings, we repeated the previous experiment, by cotransfecting pcICP22 (wt) and pcICP22-miRE-M4m, respectively, with pcDNA-mdv1-miR-M4, pcDNA-gga-miR-155 (expressing the cellular miR orthologous to mdv1-miR-M4-5p), pcDNA-mdv1-miR-M8 (expressing mdv1-premiR-M8) or native pcDNA.3.1, used as negative controls (Fig. 5b). Interestingly, an effect on ICP22 mRNA levels similar to that observed with mdv1-miR-M4 was also seen with gga-miR-155 on miRE-M4m (Fig. 5b).

We checked the impact of mdv1-miR-M4-5p and gga-miR-155-5p on ICP22 protein levels, by performing Western blots with polyclonal antiserum against ICP22 and an anti-GAPDH MAb as a control, on proteins extracted from cells cotransfected with the related miRs and miREs as previously described.

Consistent with the RT-qPCR data shown above, the presence of the ICP22 protein was found to be dependent on the simultaneous presence of mdv1-miR-M4 or gga-miR-155 and a functional miRE-M4-5p (Fig. 5c, d). Moreover, we detected no ICP22 protein in cells cotransfected with mdv1-miR-M5-3p and mdv1-miR-M1-5p (data not shown), suggesting that mdv1-miR-M4 may be required for *ICP22* expression.

ICP22 represses the expression of some viral genes

We investigated the regulation of the *ICP22* promoter by GaHV-2 proteins, by using the pcICP22, pcICP4, pcICP27 and pcVP16 constructs to cotransfect DF-1 cells with pICP22-1000 in luciferase reporter assays, with pcDNA.3.1 as a control (Fig. 6a). The ectopic expression of ICP27 and VP16 had no effect on levels of transcription from the *ICP22* promoter, whereas ICP4 and ICP22 had a significant impact, triggering an increase in promoter activity of 29% and a 52 % decrease in promoter activity, respectively (Fig. 6a).

Finally, we investigated the effect of ectopic *ICP22* expression on various viral promoters in a luciferase reporter assay on DF-1 cells cotransfected with pcICP22 and the pICP22-200, pICP27-1000, pICP4-dis, pgK-1000 and pcDNAMluc constructs, in which the promoters of *ICP22*, *ICP27*, *ICP4* and *gK* were cloned upstream from the luciferase gene of the pGL3 vector. ICP22 significantly reduced the activity of all the promoters tested, including IE promoters (pICP22-1000, pICP27-1000 and pICP4-dis), late promoters (pgK-1000) and the CMV promoter (pcDNAMluc) (Fig. 6b).

DISCUSSION

ICP22 is common to all members of the *Alphaherpesvirinae* other than Iltovirus [34]. We describe here the characteristics of the ICP22 of the oncogenic alphaherpesvirus GaHV-2, including the dependence of its expression of viral lifecycle phase. Like the ICP22s of most alphaherpesviruses, including that of HHV-1 [35], and unlike the homologous protein of HHV-3 (IE68), which is transcribed during latency [36], we confirm here, that the *ICP22* gene and the corresponding protein are expressed during the lytic and reactivation phases (Fig. 1), but not during latency as previously reported [12, 17, 37]. Moreover, we showed that the transcription profiles of *ICP22* and of the major capsid gene *VP5,* characteristic of the lytic phases of the viral cycle, are identical *in vitro,* in CEF RB-1B and in MSB-1R, and *in vivo,* in PBLs collected from RB-1B-infected chickens with high levels of expression on days 7 and 28 p.i. (initial and late lytic productive phases, respectively) (Fig. 2c), potentially corresponding to the spontaneous viral reactivation classically observed in our *in vivo* model. Finally, it should be noted that this transcription during the lytic phases of GaHV-2 infection differentiates *ICP22* from the other two ICP genes, *ICP4* and *ICP27*, which are transcribed during both lytic phases and latency [7, 26].

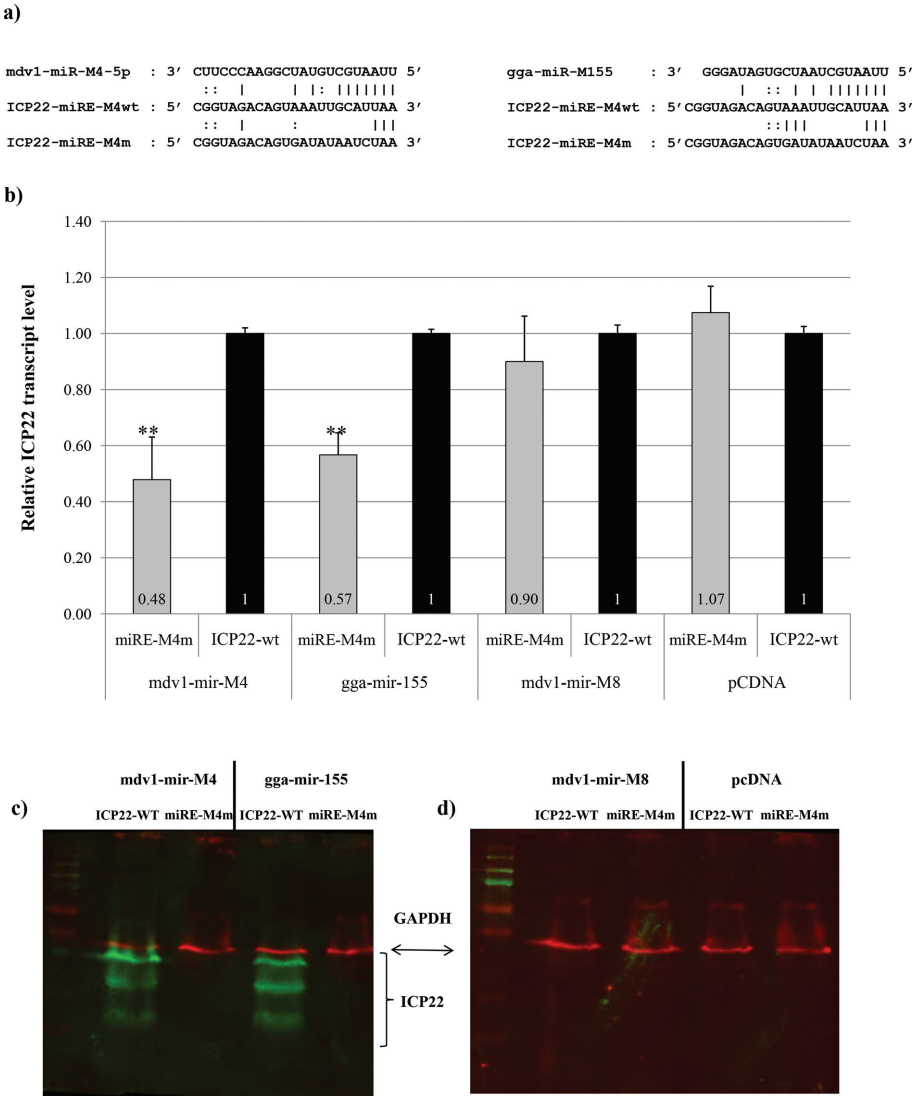

Fig. 5. Targeting of ICP22 by mdv1-miR-M4-5p. (a) The sequence complementarity of mdv1-miR-M4-5p (left) and gga-miR-155 (right) and the predicted miRE-M4wt identified in the *ICP22* sequences of the GaHV-2 RB-1B genome are shown. The microRNA seed region is highlighted in grey (: denotes wobble pair G-U, **|** denotes Watson–Crick pair); bars indicate nucleotides complementary between the miR and the corresponding miRE. ICP22-miRE-M4m is the sequence of the related mutated miRE with the changed nucleotide and complementarities. (b) Upregulation of the ICP22 transcript by mdv1-miR-M4-5p and gga-miR-155. DF-1 cells were cotransfected with pcDNA constructs pcICP22 (ICP22-wt) or pcICP22 mutated for miRE-M4-5p (miRE-M4m), and with miRNA expression vector: pcDNA-mdv1-miR-M4-5p, pcDNA-gga-miR-155, pcDNA-mdv1-miR-M8 or empty pcDNA vector as the control. Total RNA was extracted and subjected to RT-qPCR. ICP22 transcript levels were calculated relative to those of GAPDH. ICP22 mRNA levels were quantified by the RT-qPCR $2^{-\Delta\Delta Ct}$ method, with GAPDH mRNA as the reference. The histograms show the mean of triplicates of two independent lipofections of DF-1 cells. ICP22 mRNA levels were normalized relative to those obtained after transfection with pCDNA3.1. * Student's *t*-test, *P*-value<0.05 versus pCDNA3.1. (c–d) Western blot analysis of the upregulation of ICP22 by mdv1-miR-M4-5p. DF-1 cells were cotransfected with pcDNA constructs pcICP22 (ICP22-wt) or pcICP22 mutated for miRE-M4-5p (miRE-M4m), and with miRNA expression vector: pcDNA-mdv1-miR-M4-5p, pcDNA-gga-miR-155 (c), pcDNA- mdv1-miR-M8 or empty pcDNA vector as the control (d). Proteins were extracted and immunodetected with polyclonal anti-ICP22 (green) or monoclonal anti-GAPDH antibodies (red). Brackets indicate the expected position of the different forms of ICP22.

As in most alphaherpesviruses the *ICP22* genes of GaHV-2 have been shown to be located at the 5′ end of the unique short U_S region [9]. We confirmed, by 5′ and 3′ RACE, that the 1.7 kb mRNA initially identified on Northern blots and in targeted deletions contains the *ICP22* transcript [11, 13]. We characterized this mRNA as a 1587 nt bicistronic transcript (from TSS_{155440} to the beginning of the polyA domain, positions 155442 and 157089, respectively)

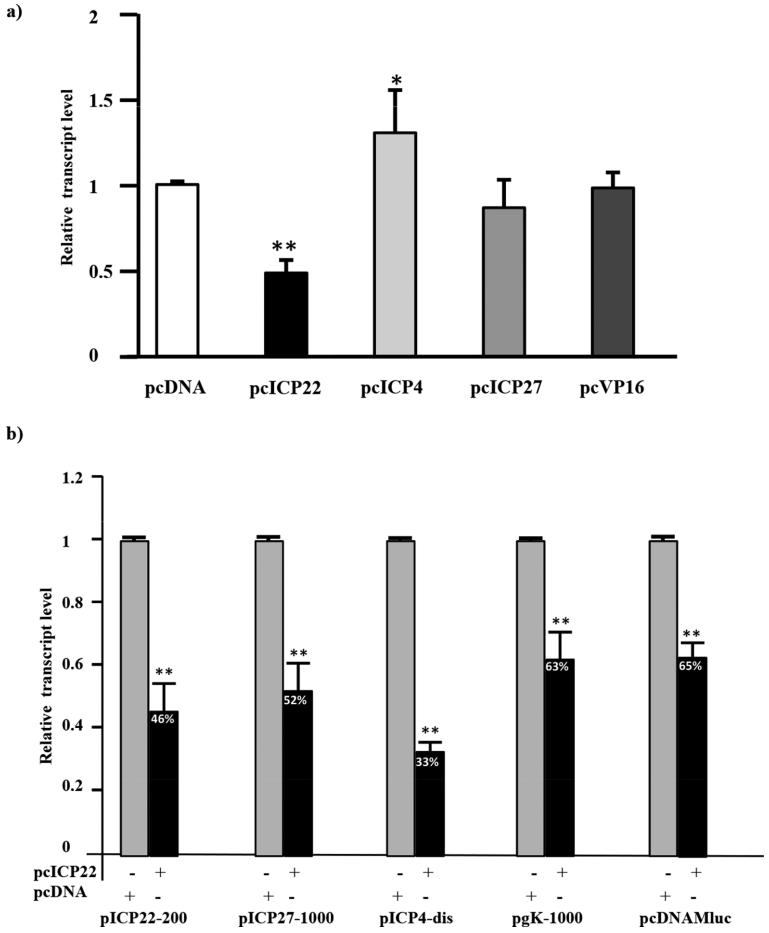

Fig. 6. Impact of ectopically expressed GaHV-2 immediate early proteins on IE and L genes' promoter activity. (a) DF-1 cells were cotransfected with the pICP22-200 reporter vector with the pcDNA ICP expression vector (pcICP22, pcICP4, pcICP27), the pcDNA VP16 expression vector (pcVP16) or an empty pcDNA3.1 vector. Promoter activities were normalized with respect to the corresponding empty pcDNA3.1 vector (standardized to 1). (b) Effect of ICP22 ectopic expression by cotransfection of pcICP22 with pGL3 plasmids containing the promoter sequences of ICP22, ICP27, ICP4 and gk (pICP22-200, pICP27-1000, pICP4-dis, pgK-1000) in DF-1 cells. Error bars indicate the SEM for three independent biological experiments performed in triplicate (n=3). (**) indicates significant values P<0.05 in Student's t-test.

encompassing the *ICP22* and *US10* genes (Fig. 2a). Our data suggest that *ICP22* and *US10* share an AATAAA polyadenylation signal downstream from the *US10* gene (position 157010) [12, 13]. This sharing of a single polyadenylation signal by more than one gene, which is very common in alphaherpesviruses, has already been reported for the U_S and U_L regions of GaHV-2, for the *US7* (*gI*), and *US8* (*gE*), *UL53* (*gK*) and *UL54* (*ICP27*) genes, respectively [26, 38]. In addition, a previous study showed that two other mRNAs (2.6 and 0.9 kb) transcribed from the 5′ region of U_S are more weakly detected than the 1.7 kb mRNA by a probe covering the *ICP22* and *US10* genes [12]. By 5′ RACE specific for the *SORF2* and *US10* genes on RNA extracted from RB-1B CEFs and *n*-butyrate-treated MSB-1 cells, we also identified two major TSSs, 128 nt (position 154647) and 55 nt (position 156254) upstream from the two genes, respectively. The use of these sites, together with the 157010-AATAAA polyadenylation would lead to the production of mRNA molecules of 2360 nt and 780 nt in length (data not shown). However, we can not exclude that the 0.9 kb mRNA instead could correspond to a weakly expressed monocistronic ICP22 mRNA of 849 nt, beginning at the TSS_{155440} and ending at the lower efficiency polyadenylation signal 156289-ATTAAA site, which we have found to be very poorly functional.

The transcription of both mono- and bicistronic *ICP22* mRNAs is driven by a single promoter, including a core promoter located within the 200 nt immediately upstream from TSS_{155440}. These characteristics are consistent with the description of classical major IE herpesvirus promoters, which commonly include functional ubiquitous REs, such as CRE, TATA and GC boxes [39]. In addition, the three most effective REs – the GATA box, E-box and ETS-1 REs

– mutations of which reduced luciferase activity by up to 50 % (Fig. 3b), have classically been implicated in lymphomagenesis and the viral infection of lymphocytes. In particular, the transactivator ETS-1 is essential for lymphangiogenesis due to HHV8 and for EBV HHV4 lymphomagenesis [40, 41]. Together with USF-1, it is involved in the transcriptional activity of HIV in T lymphocytes [42]. In addition, ICP4 is the only one of the four overexpressed viral transactivators to enhance *ICP22* transcription significantly, consistent with a role as a major early activator. As observed for the other two ICPs of GaHV-2 (*ICP4* and *ICP27*) [7, 26], the absence of an effect of the VP16 of GaHV-2 on the transcription of *ICP22* provides support for a non-essential role of this protein in virus growth *in vitro* [43].

Unlike the other two GaHV-2 ICP genes, which are regulated by dual promoters at the transcriptional level and by alternative splicing at the posttranscriptional level [7, 26], expression of the GaHV-2 *ICP22* gene is regulated by a single promoter, to generate an unspliced transcript. Contrasting again with *ICP27* and *ICP4*, the viral phase-dependent expression of *ICP22* seems to be unrelated to the methylation level of the promoter (Fig. 3c). The light methylation of the *ICP22* promoter, regardless of viral cycle phase, is consistent with published data reporting only weak methylation of this genomic region of GaHV-2 [17, 44]. As no methylation was detected during latency, and only the E-box was slightly methylated during the reactivation or lytic phases when ICP22 is transcribed, epigenetic methylation may be involved in fine-tuning the expression of *ICP22* during lytic infection or reactivation.

Conversely, miR-mediated epigenetic regulation of *ICP22* expression seems to be essential. Two viral miRs, expressed more strongly in tumours than in GaHV-2-infected CEFs [45], mdv1-miR-M1-5P and mdv1-miR-M5-3P, had typical effects. The binding of these two miRs to their miREs in the ORF, decreased ICP22 mRNA levels by a factor of about 2.5 in DF-1 transfected cells (Fig. 4). By contrast, in a similar experiment, the binding of mdv1-miR-M4-5P and of the orthologous cellular miR gga-mir-155-3p to the stop codon overlapping miRE-M4 leads to an increase in ICP22 mRNA levels, and would be strictly required for production of the protein in productive cells (Fig. 5). We suggest, that in latently infected MSB-1 lymphocytes, the effect of mdv1-miR-M4-5p could be abolished by mdv1-miR-M1-5P and especially the strong expression of mdv1-miR-M5-3p (Figs 1b and 4b). These last two miRs, may also fine-tune *ICP22* expression during the lytic phases of the infection and in GaHV-2-infected CEFs, in which they are weakly expressed. Finally, these data add to those of our previous studies, showing that mdv1-miR-M7-5p and mdv1-miR-M4-5P target the other two GaHV-2 ICP genes (*ICP4* and *ICP27*) and two late genes (*UL28* and *UL32*), respectively, demonstrating the ability of viral miRs to regulate both the latent and lytic phases of the lifecycle [26, 29].

An analysis of all published miR libraries, in which mdv1-miR-M4-5P is one of the two most strongly expressed miRs both during lytic phases and latency [45–48], strongly suggested that this molecule is a key miR for GaHV-2 replication *in vivo* and *in vitro*. In addition, a previous study showed that mutations of the mdv1-miR-M4 seed sequence led a loss of GaHV-2 oncogenicity, and that mdv1-miR-M4-5P could be replaced by gga-mir-155 in the viral genome with no significant effect on tumour induction [30]. Moreover, the authors reported that oncogenesis required the presence of other miRs from the mdv1-miR-M4-M9 cluster, such as mdv1-miR-M5. However, as mdv1-miR-M4-5P accounts for 70 % of the viral miRs expressed *in vivo* in libraries established from PBLs and feather follicles of chickens infected with the non-oncogenic strain CVI-988 (data not shown), we suggest that it probably also plays a major role in the lytic phase of GaHV-2, possibly by upregulating ICP22.

We were able to identify only two published examples of translational enhancement resulting from the direct interaction of a miR with the targeted mRNA. Specifically, the binding of hsa-miR-10a and hsa-miR-122 to their miRE in the 5′-UTR region of ribosomal proteins and of the HCV genome, respectively, allows translation [49, 50]. Our model, in which the binding of mdv1-miR-M4-5P and gga-mir-155-3P to the ICP22 stop codon affects both the amount of mRNA produced and its translation, seems to correspond instead to a possible new example of nonsense-mediated mRNA decay (NMD)-based immunity. NMD was initially described as an RNA surveillance mechanism responsible for eliminating aberrant transcripts containing premature termination codons (PTCs), but it is also involved in the regular negative control of 3 to 20 % of genes [51]. The presence of ORFs in the 3′-UTR or an atypically long 3′-UTR facilitates the downregulation of these normal mRNAs by NMD. A bioinformatic analysis of the human RefSeq transcriptome showed that only a few unspliced bicistronic eukaryotic transcripts are translated, and that these transcripts use various strategies to escape NMD [52]. We suggest that the unspliced bicistronic transcript of *ICP22*, which contains a long 3′-UTR encompassing the US10 ORF, is likely to be controlled by NMD (Fig. 2). In addition, based on our data, showing that the translation of ICP22 from the monocistronic construct (pICP22) is also dependent on mdv1-miR-M4-5P or gga-mir-155-3P (Fig. 5), we presume that the binding of mdv1-miR-M4-5P/Ago2 to the stop codon would increase mRNA levels, making it possible to generate ICP22 protein. These hypotheses are currently being tested, by assessing the stabilization of NMD-targeted cellular transcripts by miR-mediated gene silencing through microarray approaches that have identified 45 monocistronic and nine bicistronic transcripts of HeLa cells displaying downregulation, by a factor of two to three, on Ago2 silencing [53]. Moreover, the binding of the miR/Ago2 complex close to the stop codon would result in a direct interaction of Ago2 with the cap, leading directly to eIF4E-dependent translation without the pre-scanning by

CBP80/20-dependent translation classically observed during nuclear mRNA export [53].

We showed, by expressing *ICP22* ectopically in DF-1 cells not infected with GaHV-2, that the GaHV-2 ICP22 downregulates the transcriptional activity of the five promoters tested: its own promoter, the promoters of the two IE genes *ICP27* and *ICP4*, and those of *gK* and CMV present in pcDNAMluc (Fig. 6b). These data are consistent with findings for HHV-1, HHV-3, SuHV-1 and BoHV-2 [16, 21, 54–56], showing that ICP22 decreases the transcription of genes in a cell type-specific manner, possibly by regulating the phosphorylation of RNA polymerase II, as in HHV-1 [35]. This intrinsic function, which is conserved among herpesvirus ICP22 proteins, is supported by an alignment of the corresponding protein, which showed there to be 36 % identity in the IE_68 domain (Fig. S1, available in the online version of this article). In addition, the ICP22 of mardiviruses is shorter than that of the other alphaherpesviruses [10]. It consists essentially of the IE_68 domain, without the long NH_2 and COOH terminal repeat sequences carrying the nuclear localization signals found in other alphaherpesviruses which drive the nuclear localization of ICP22 in the HHV-1, HHV-3 and SuHV-1 models [57–61]. These observations may reflect former findings, confirming here that the ICP22 protein is detectable mainly in the cytoplasm of GaHV-2-infected cells (Fig. 1a) despite its transactivator activity, suggesting that ICP22 is imported to the nucleus independently of the presence of an NLS [12, 17]. Such observations have also been described for ICP4 and for the viral phosphorylated GaHV-2 pp38, ICP22 appearing associated to pp38 at distinct cytoplasmic sites [7, 12, 17]. Several NLS-independent mechanisms may mediate nuclear import [59]: transport through alternative carriers, as reported for the transport of the VP5 of HHV-1 by VP22a [58], direct nuclear import through passive diffusion for proteins with molecular mass of up to 40 kDa [59] or phosphorylation/dephosphorylation coupled to translocation to the nucleus with an NLS-independent mechanism may account for ICP22 nuclear import [56, 60]. Finally, we cannot rule out that a small undetectable amount of ICP22 is imported to the nucleus at a rate driving promoter activity. Further investigations are required to precisely establish the mechanism whereby GaHV-2 ICP22 is transported into the nucleus.

In conclusion, we studied the transcriptional and posttranscriptional regulation of *ICP22,* the third and last GaHV-2 ICP gene. *ICP22* is expressed exclusively during the lytic phases of viral infection *in vivo* and *in vitro*. This pattern of regulation contrasts strongly with that of the other two ICPs. The transcription of the unspliced *ICP22* mRNA is driven by a single promoter that is not regulated by methylation. As observed for ICP4 and ICP27, the expression of ICP22 is regulated by viral miRs. However, whereas mdv1-miR-M1-5P and mdv1-miR-M5-3p act like mdv1-miR-M7-5P for ICP4 and ICP27, reducing the level of *ICP22* mRNA, the binding of mdv1-miR-M4-5P to the stop codon seems to be required for production of the ICP22 protein. Finally, we propose a very preliminary model, in which *ICP22* expression is promoted initially by the expression of gga-mir-155-3P in PBLs and then by mdv1-miR-M4-5P in infected PBLs, in which gga-mir-155-3P is repressed [29]. As shown for HHV-1 [61], ICP22 could shut off the transcription of cellular genes during the lytic phase and reactivation. As mdv1-miR-M4-5P is strongly expressed during all phases of infection, *ICP22* would be repressed by RNA interference due to mdv1-miR-M1-5P and the overexpressed mdv1-miR-M5-3P during latency, allowing latently infected cells to survive. Further studies are currently underway to confirm this putative model and to increase our understanding of the fine mechanism involved in the direct positive epigenetic regulation of a protein by a single miR.

METHODS

Virus strain and cell cultures

The latently infected MSB-1 cell line, derived from a spleen lymphoma induced by a virulent strain of GaHV-2 [62], was maintained in RPMI 1640 medium (Lonza) supplemented with 1 mM sodium pyruvate, 10 % fetal bovine serum, and 5 % chicken serum. Viral reactivation from latency was induced with 3 mM n-butyrate, as previously described [25]. DF-1 cells, obtained from a chicken fibroblast cell line, were cultured in a similar manner, in Dulbecco's modified Eagle's medium (DMEM) supplemented with 10 % fetal calf serum (FCS) and 5 % chicken serum (CS). Chicken embryo fibroblasts (CEFs) were maintained in DMEM (Lonza) supplemented with 2.5 % FCS, 1.25 % CS, 1 % penicillin/streptomycin, 1 % amphotericin B (Fungizone) and 5 % tryptose phosphate broth (TPB). CEFs were prepared for propagation of the RB-1B virus strain, as previously described [63].

RACE-PCR and RT-PCR analysis

For RACE-PCR, total RNA was isolated with Trizol (Invitrogen) from reactivated MSB-1 (MSB-1R) or CEF RB-1B cells, according to the manufacturer's instructions, and was treated with DNase (Promega). The cDNA ends were amplified from 5 µg of RNA, with a GeneRacer kit (Invitrogen), according to the manufacturer's instructions, and with the primers shown in Table S1. Each 5′ and 3′ RACE-PCR was performed as a nested-RACE-PCR with gene-specific and nested gene-specific primers binding to sites a short distance apart (Fig. 2, Table S1).

For RT-PCR analysis, total RNA was isolated and cDNA ends were amplified with the RNA+extraction kit (Macherey-Nagel), according to the manufacturer's instructions, using the primers shown in Table S1. For RT-PCR, we reverse-transcribed 0.5 µg of RNA with a mixture of oligo (dT) and random primers (Eurogentec) and the Superscript-III reverse transcriptase (Invitrogen). The efficacy of the DNase treatment of RNA was systematically confirmed by PCR. A negative control for reverse transcription (RT-) was systematically performed in the same

conditions. The cDNAs generated were amplified by PCR with the GoTaq DNA polymerase (Promega), according to the manufacturer's instructions, and with the primers listed in Table S1. The cDNAs from PBLs (peripheral blood leukocytes) have been described elsewhere [64].

For RACE-PCR and RT-PCR, the PCR products were inserted into pGEM-T Easy (Promega) and sequenced by GATC Biotech. All sequences were analysed by comparison with the viral RB-1B sequence (GenBank accession number RB-1B EF523390), with Geneious software (www.geneious.com) and BLAST.

Quantitative RT-PCRs

To quantify ICP22 mRNA, mdv1-miR-M1-5p, mdv1-miR-M4-5p and mdv1-miR-M5-3p expression levels (primers shown in Table S1) *via* the $2^{-\Delta\Delta\ Ct}$ method, the miScript PCR System (Qiagen) was used. One microgram of total RNA from CEF RB-1B, MSB-1 and MSB-1R cells was reverse-transcribed using the miScript II RT Kit (Qiagen) in a total volume of 20 µl, and 2 µl of a 1 : 10 dilution was used for quantitative PCR, as recommended by the manufacturer (Applied Biosystems). Glyceraldehyde-3-phosphate dehydrogenase (GAPDH; primers shown in Table S1) and U6 (miScript; Qiagen) were used as reference genes for ICP22 and mdv1-miR experiments. All q-PCRs were performed on the StepOnePlus Real-time PCR System (Applied Biosystems) following the conditions recommended by the manufacturer, and dissociation curves were generated post-run.

Plasmid constructs

For the pGL3 luciferase reporter constructs, all the putative promoter sequences were amplified with the primer pairs described in Table S1 and inserted into the pGL3-Basic vector (Promega), as previously described [26].

The plasmids were purified with the NucleoBond Xtra Midi kit (Macherey-Nagel), and the sequences of all inserts from each construct were systematically verified (GATC Biotech).

The pGL3 plasmid, containing the promoter sequences of ICP27 (pICP27-1000), ICP4 (pICP4-dis) and gk (pgk-1000), was generated in previous studies [26, 62].

For the pcDNA3.1 expression contructs, the 540 bp ICP22 gene was first amplified by PCR from CEF RB-1B, with the primer pairs indicated in Table S1. It was inserted into the pGEMT-easy vector (Promega), and introduced into the pcDNA3.1 vector (pcICP22) (Table S1). pcICP27 and pcICP4 were produced in previous studies [7, 33]. pcICP22 vectors with mutations of the mdv1-miR-M1-5p, mdv1-miR-M5-3p and mdv1-miR-M4-5p target sites were constructed by overlapping PCR (Table S1), from the pcICP22 vector (Table S1). The resulting amplicon was inserted into the pcDNA3 expression vector to generate pcICP22-miRE-M1m, pcICP22-miRE-M5m and pcICP22-miRE-M4m.

Dual luciferase reporter assays

Luciferase activity with pGL3 promoter constructs was quantified with the dual-luciferase reporter assay system (Promega), using one million MSB-1 cells transfected with 100 ng of pGL3 reporter construct, according to the manufacturer's protocol. For the inter- and intra-assay standardization of luciferase activity, we systematically used 60 ng of the control vector pCDNA-MLuc, from which the firefly luciferase gene is expressed under the control of the CMV promoter, and 2 mg pRL-TK *Renilla* luciferase reporter construct carrying the *Renilla* luciferase gene under the control of the thymidine kinase promoter of HHV-1 [29]. Firefly and *Renilla* luciferase activities were measured consecutively 24 h after transfection. Luminescence was measured with a luminometer (Tristar^2 luminometer; Berthold Technologies). Three independent experiments were carried out in triplicate. Student's *t*-test was used for statistical analysis.

The effects of ICP22 on IE promoters and the effects of IE proteins on the *ICP22* promoter were tested in adherent DF-1 cells, plated in six-well dishes at a density of 5×10^5 cells per well, and cotransfected in the presence of Lipofectamine 2000 (Invitrogen) with 500 ng of the promoter-luciferase reporter vector, and 500 ng of the pcDNA3.1-ICP expression vector or an empty pcDNA3.1 vector. Promoter activities were normalized with respect to the corresponding empty pcDNA3.1 (standardized to 1).

DNA isolation, bisulfite (BS) treatment and PCR

DNA was isolated with the DNeasy Blood and Tissue Kit (Qiagen). BS treatment was performed with the EZ DNA methylation – gold kit (Zymo Research), which converts unmethylated cytosine residues into uracils, which are then converted into thymidine residues during PCR. Nested PCR was then performed with the primers indicated in Table S1, with the Epimark Hot-Start *Taq* DNA polymerase (New England Biolabs). Amplicons were inserted into the pGEM-T easy vector (Promega) and the DNA insert was sequenced.

Detection of ICP22 transcript and protein after transient miR expression

Adherent DF-1 cells, plated in six-well dishes at a density of 5×10^5 cells per well, were cotransfected in the presence of Lipofectamine 2000 (Invitrogen) with 500 ng pcICP22, pcICP22-miRE-M1m, pcICP22-miRE-M5m and pcICP22-miRE-M4m and 25 ng pcDNA-mdv1-miR-M1, pcDNA-mdv1-miR-M5, pcDNA-mdv1-miR-M4, pcDNA-mdv1-miR-M8 or pcDNA-gga-miR-M155.

We used the Power SYBR Green Master system (Applied Biosystems) to quantify ICP22 mRNA levels by the $2^{-\Delta\Delta Ct}$ method. We subjected 1 µg of extracted RNA to reverse transcription in a total volume of 20 µl, and 2 µl of a 1 : 10 dilution was used for quantitative PCR with specific primers, as indicated by the manufacturer (Table S1). GAPDH was used as the reference gene. All qPCRs were performed on the StepOnePlus Real-time PCR System (Applied Biosystems), in the conditions recommended by the manufacturer, and dissociation curves were generated post-run.

Cells were lysed 24 h after transfection, and the proteins were separated electrophoretically and blotted onto nitrocellulose membranes. The membranes were blocked by incubation with blocking buffer (Odyssey) and probed with a rabbit polyclonal anti-ICP22 antibody or mouse anti-GAPDH antibody, followed by monoclonal goat anti-rabbit or anti-mouse infrared dye (IRD)-labelled secondary antibodies (Odyssey). The immunoreactions of interest were detected after excitation with light at wavelengths of 700 and 800 nm for the anti-mouse and anti-rabbit antibodies, respectively. Protein levels were normalized with respect to the corresponding empty pcDNA3.1 (standardized to 1).

Immunofluorescence

ICP22 proteins from CEF RB-1B and MSB-1 cells previously spotted with a Cytospin apparatus (Shandon, Thermo Scientific), were detected with rabbit polyclonal anti-ICP22 antibodies. VP5 proteins were detected with the mouse anti-vp5 mAb diluted 1 : 200.

Funding information
This work was supported by grants from the Ligue contre le Cancer Grand Ouest-Comités (18, 29, 35, 36 and 37). S. P. is a 'Fonds Pour la formation à la recherche dans l'industrie et dans l'agriculture' (FRIA) PhD fellow (Belgium). We thank 'Campus Fance' and 'Le consulat de France au Maroc' for having supported financialy Imane Boumart.

Conflicts of interest
The authors declare that there are no conflicts of interest.

References

1. **Cantello JL, Anderson AS, Morgan RW.** Identification of latency-associated transcripts that map antisense to the ICP4 homolog gene of Marek's disease virus. *J Virol* 1994;68:6280–6290.
2. **Burnside J, Bernberg E, Anderson A, Lu C, Meyers BC *et al.*** Marek's disease virus encodes MicroRNAs that map to meq and the latency-associated transcript. *J Virol* 2006;80:8778–8786.
3. **Calnek BW.** Pathogenesis of Marek's disease virus infection. *Curr Top Microbiol Immunol* 2001;255:25–55.
4. **Schat KA NV.** *Marek's Disease*. Wiley-Blackwell Publishers; 2013.
5. **Wu CL, Wilcox KW.** The conserved DNA-binding domains encoded by the herpes simplex virus type 1 ICP4, pseudorabies virus IE180, and varicella-zoster virus ORF62 genes recognize similar sites in the corresponding promoters. *J Virol* 1991;65:1149–1159.
6. **White K, Peng H, Hay J, Ruyechan WT.** Role of the IE62 consensus binding site in transactivation by the varicella-zoster virus IE62 protein. *J Virol* 2010;84:3767–3779.
7. **Rasschaert P, Gennart I, Boumart I, Dambrine G, Muylkens B *et al.*** Specific transcriptional and post-transcriptional regulation of the major immediate early ICP4 gene of GaHV-2 during the lytic, latent and reactivation phases. *J Gen Virol* 2018:355–368.
8. **Deluca N.** Functions and mechanism of action of the herpes simplexvirus regulatory protein ICP4. *Alphaherpesviruses*. Norfolk, UK: Weller SK; 2011. pp. 17–38.
9. **Brunovskis P, Velicer LF.** The Marek's disease virus (MDV) unique short region: alphaherpesvirus-homologous, fowlpox virus-homologous, and MDV-specific genes. *Virology* 1995;206:324–338.
10. **Li ML, Chen JH, Zhao ZY, Zhang KJ, Li Z *et al.*** Molecular cloning and characterization of the pseudorabies virus US1 gene. *Genet Mol Res* 2013;12:85–98.
11. **Schat KA, Buckmaster A, Ross LJ.** Partial transcription map of Marek's disease herpesvirus in lytically infected cells and lymphoblastoid cell lines. *Int J Cancer* 1989;44:101–109.
12. **Parcells MS, Anderson AS, Morgan TW.** Retention of oncogenicity by a Marek's disease virus mutant lacking six unique short region genes. *J Virol* 1995;69:7888–7898.
13. **Parcells MS, Anderson AS, Cantello JL, Morgan RW.** Characterization of Marek's disease virus insertion and deletion mutants that lack US1 (ICP22 homolog), US10, and/or US2 and neighboring short-component open reading frames. *J Virol* 1994;68:8239–8253.
14. **Tombácz D, Tóth JS, Petrovszki P, Boldogkoi Z.** Whole-genome analysis of pseudorabies virus gene expression by real-time quantitative RT-PCR assay. *BMC Genomics* 2009;10:491.
15. **Schwyzer M, Wirth UV, Vogt B, Fraefel C.** BICP22 of bovine herpesvirus 1 is encoded by a spliced 1.7 kb RNA which exhibits immediate early and late transcription kinetics. *J Gen Virol* 1994;75:1703–1711.
16. **Köppel R, Vogt B, Schwyzer M.** Immediate-early protein BICP22 of bovine herpesvirus 1 trans-represses viral promoters of different kinetic classes and is itself regulated by BICP0 at transcriptional and posttranscriptional levels. *Arch Virol* 1997;142:2447–2464.
17. **Parcells MS, Dienglewicz RL, Anderson AS, Morgan RW.** Recombinant Marek's disease virus (MDV)-derived lymphoblastoid cell lines: regulation of a marker gene within the context of the MDV genome. *J Virol* 1999;73:1362–1373.
18. **Rice SA, Long MC, Lam V, Schaffer PA, Spencer CA.** Herpes simplex virus immediate-early protein ICP22 is required for viral modification of host RNA polymerase II and establishment of the normal viral transcription program. *J Virol* 1995;69:5550–5559.
19. **Purves FC, Ogle WO, Roizman B.** Processing of the herpes simplex virus regulatory protein alpha 22 mediated by the UL13 protein kinase determines the accumulation of a subset of alpha and gamma mRNAs and proteins in infected cells. *Proc Natl Acad Sci USA* 1993;90:6701–6705.
20. **Bowman JJ, Orlando JS, Davido DJ, Kushnir AS, Schaffer PA.** Transient expression of herpes simplex virus type 1 ICP22 represses viral promoter activity and complements the replication of an ICP22 null virus. *J Virol* 2009;83:8733–8743.
21. **Takács IF, Tombácz D, Berta B, Prazsák I, Póka N *et al.*** The ICP22 protein selectively modifies the transcription of different kinetic classes of pseudorabies virus genes. *BMC Mol Biol* 2013;14:2.
22. **Jackers P, Defechereux P, Baudoux L, Lambert C, Massaer M *et al.*** Characterization of regulatory functions of the varicella-zoster virus gene 63-encoded protein. *J Virol* 1992;66:3899–3903.
23. **Holden VR, Zhao Y, Thompson Y, Caughman GB, Smith RH *et al.*** Characterization of the regulatory function of the ICP22 protein of equine herpesvirus type 1. *Virology* 1995;210:273–282.
24. **Kato K, Izumiya Y, Tohya Y, Takahashi E, Hirai K *et al.*** Identification and characterization of Marek's disease virus serotype 1 (MDV1) ICP22 gene product: MDV1 ICP22 transactivates the MDV1 ICP27 promoter synergistically with MDV1 ICP4. *Vet Microbiol* 2002;85:305–313.
25. **Strassheim S, Stik G, Rasschaert D, Laurent S.** mdv1-miR-M7-5p, located in the newly identified first intron of the latency-associated transcript of Marek's disease virus, targets the immediate-early genes ICP4 and ICP27. *J Gen Virol* 2012;93:1731–1742.
26. **Strassheim S, Gennart I, Muylkens B, André M, Rasschaert D *et al.*** Oncogenic Marek's disease herpesvirus encodes an isoform of the conserved regulatory immediate early protein ICP27 generated by alternative promoter usage. *J Gen Virol* 2016;97:2399–2410.
27. **Sorel O, Dewals BG.** MicroRNAs in large herpesvirus DNA genomes: recent advances. *Biomol Concepts* 2016;7:229–239.
28. **Zhao Y, Yao Y, Xu H, Lambeth L, Smith LP *et al.*** A functional MicroRNA-155 ortholog encoded by the oncogenic Marek's disease virus. *J Virol* 2009;83:489–492.
29. **Muylkens B, Coupeau D, Dambrine G, Trapp S, Rasschaert D.** Marek's disease virus microRNA designated Mdv1-pre-miR-M4 targets both cellular and viral genes. *Arch Virol* 2010;155:1823–1837.

30. Zhao Y, Xu H, Yao Y, Smith LP, Kgosana L *et al.* Critical role of the virus-encoded microRNA-155 ortholog in the induction of Marek's disease lymphomas. *PLoS Pathog* 2011;7:e1001305.
31. Jochum S, Ruiss R, Moosmann A, Hammerschmidt W, Zeidler R. RNAs in Epstein-Barr virions control early steps of infection. *Proc Natl Acad Sci USA* 2012;109:E1396–E1404.
32. Grey F, Tirabassi R, Meyers H, Wu G, McWeeney S *et al.* A viral microRNA down-regulates multiple cell cycle genes through mRNA 5'UTRs. *PLoS Pathog* 2010;6:e1000967.
33. Amor S, Strassheim S, Dambrine G, Remy S, Rasschaert D *et al.* ICP27 protein of Marek's disease virus interacts with SR proteins and inhibits the splicing of cellular telomerase chTERT and viral vIL8 transcripts. *J Gen Virol* 2011;92:1273–1278.
34. Rice SA, Davido DJ. HSV-1 ICP22: hijacking host nuclear functions to enhance viral infection. *Future Microbiol* 2013;8:311–321.
35. Kennedy PG, Rovnak J, Badani H, Cohrs RJ. A comparison of herpes simplex virus type 1 and varicella-zoster virus latency and reactivation. *J Gen Virol* 2015;96:1581–1602.
36. Yamaguchi T, Kaplan SL, Wakenell P, Schat KA. Transactivation of latent Marek's disease herpesvirus genes in QT35, a quail fibroblast cell line, by herpesvirus of turkeys. *J Virol* 2000;74:10176–10186.
37. McGeoch DJ, Dolan A, Donald S, Rixon FJ. Sequence determination and genetic content of the short unique region in the genome of herpes simplex virus type 1. *J Mol Biol* 1985;181:1–13.
38. Weir JP. Regulation of herpes simplex virus gene expression. *Gene* 2001;271:117–130.
39. Gutierrez KD, Morris VA, Wu D, Barcy S, Lagunoff M. Ets-1 is required for the activation of VEGFR3 during latent Kaposi's sarcoma-associated herpesvirus infection of endothelial cells. *J Virol* 2013;87:6758–6768.
40. Baran-Marszak F, Fagard R, Girard B, Camilleri-Broët S, Zeng F *et al.* Gene array identification of Epstein Barr virus-regulated cellular genes in EBV-converted Burkitt lymphoma cell lines. *Lab Invest* 2002;82:1463–1479.
41. Sieweke MH, Tekotte H, Jarosch U, Graf T. Cooperative interaction of ets-1 with USF-1 required for HIV-1 enhancer activity in T cells. *Embo J* 1998;17:1728–1739.
42. Dorange F, Tischer BK, Vautherot JF, Osterrieder N. Characterization of Marek's disease virus serotype 1 (MDV-1) deletion mutants that lack UL46 to UL49 genes: MDV-1 UL49, encoding VP22, is indispensable for virus growth. *J Virol* 2002;76:1959–1970.
43. Brown AC, Nair V, Allday MJ. Epigenetic regulation of the latency-associated region of Marek's disease virus in tumor-derived T-cell lines and primary lymphoma. *J Virol* 2012;86:1683–1695.
44. Burnside J, Morgan RW. Genomics and Marek's disease virus. *Cytogenet Genome Res* 2007;117:376–387.
45. Yao Y, Zhao Y, Xu H, Smith LP, Lawrie CH *et al.* MicroRNA profile of Marek's disease virus-transformed T-cell line MSB-1: predominance of virus-encoded microRNAs. *J Virol* 2008;82:4007–4015.
46. Stik G, Muylkens B, Coupeau D, Laurent S, Dambrine G *et al.* Small RNA cloning and sequencing strategy affects host and viral microRNA expression signatures. *J Biotechnol* 2014;181:35–44.
47. Burnside J, Ouyang M, Anderson A, Bernberg E, Lu C *et al.* Deep sequencing of chicken microRNAs. *BMC Genomics* 2008;9:185.
48. Ørom UA, Nielsen FC, Lund AH. MicroRNA-10a binds the 5'UTR of ribosomal protein mRNAs and enhances their translation. *Mol Cell* 2008;30:460–471.
49. Machlin ES, Sarnow P, Sagan SM. Masking the 5' terminal nucleotides of the hepatitis C virus genome by an unconventional microRNA-target RNA complex. *Proc Natl Acad Sci USA* 2011;108:3193–3198.
50. He F, Jacobson A. Nonsense-mediated mRNA decay: degradation of defective transcripts is only part of the story. *Annu Rev Genet* 2015;49:339–366.
51. Shahaf G, Shweiki D. Nonsense-mediated mRNA decay immunity can help identify human polycistronic transcripts. *PLoS One* 2014;9:e91535.
52. Choe J, Cho H, Chi SG, Kim YK. Ago2/miRISC-mediated inhibition of CBP80/20-dependent translation and thereby abrogation of nonsense-mediated mRNA decay require the cap-associating activity of Ago2. *FEBS Lett* 2011;585:2682–2687.
53. Jones C. Herpes simplex virus type 1 and bovine herpesvirus 1 latency. *Clin Microbiol Rev* 2003;16:79–95.
54. Hoover SE, Cohrs RJ, Rangel ZG, Gilden DH, Munson P *et al.* Downregulation of varicella-zoster virus (VZV) immediate-early ORF62 transcription by VZV ORF63 correlates with virus replication in vitro and with latency. *J Virol* 2006;80:3459–3468.
55. Habran L, El Mjiyad N, Di Valentin E, Sadzot-Delvaux C, Bontems S *et al.* The varicella-zoster virus immediate-early 63 protein affects chromatin-controlled gene transcription in a cell-type dependent manner. *BMC Mol Biol* 2007;8:99.
56. Stelz G, Rücker E, Rosorius O, Meyer G, Stauber RH *et al.* Identification of two nuclear import signals in the alpha-gene product ICP22 of herpes simplex virus 1. *Virology* 2002;295:360–370.
57. Cai M, Jiang S, Zeng Z, Li X, Mo C *et al.* Probing the nuclear import signal and nuclear transport molecular determinants of PRV ICP22. *Cell Biosci* 2016;6:3.
58. Nicholson P, Addison C, Cross AM, Kennard J, Preston VG *et al.* Localization of the herpes simplex virus type 1 major capsid protein VP5 to the cell nucleus requires the abundant scaffolding protein VP22a. *J Gen Virol* 1994;75:1091–1099.
59. Wagstaff KM, Jans DA. Importins and beyond: non-conventional nuclear transport mechanisms. *Traffic* 2009;10:1188–1198.
60. Walters MS, Kyratsous CA, Wan S, Silverstein S. Nuclear import of the varicella-zoster virus latency-associated protein ORF63 in primary neurons requires expression of the lytic protein ORF61 and occurs in a proteasome-dependent manner. *J Virol* 2008;82:8673–8686.
61. Rivas HG, Schmaling SK, Gaglia MM. Shutoff of host gene expression in influenza A virus and herpesviruses: similar mechanisms and common themes. *Viruses* 2016;8:102.
62. Figueroa T, Boumart I, Coupeau D, Rasschaert D. Hyperediting by ADAR1 of a new herpesvirus lncRNA during the lytic phase of the oncogenic Marek's disease virus. *J Gen Virol* 2016;97:2973–2988.
63. Coupeau D, Dambrine G, Rasschaert D. Kinetic expression analysis of the cluster mdv1-mir-M9-M4, genes meq and vIL-8 differs between the lytic and latent phases of Marek's disease virus infection. *J Gen Virol* 2012;93:1519–1529.
64. Debba-Pavard M, Ait-Lounis A, Soubieux D, Rasschaert D, Dambrine G. Vaccination against Marek's disease reduces telomerase activity and viral gene transcription in peripheral blood leukocytes from challenged chickens. *Vaccine* 2008;26:4904–4912.